RESEARCH ARTICLE | SEPTEMBER 06 2023

Interface charge engineering on an *in situ* SiN_x/AlGaN/GaN platform for normally off GaN MIS-HEMTs with improved breakdown performance

JiaQi He ; KangYao Wen ; PeiRan Wang ; MingHao He ; FangZhou Du ; Yang Jiang ; ChuYing Tang ; Nick Tao ; Qing Wang ; Gang Li ; HongYu Yu

Appl. Phys. Lett. 123, 103502 (2023)
https://doi.org/10.1063/5.0169944

Interface charge engineering on an *in situ* SiN_x/AlGaN/GaN platform for normally off GaN MIS-HEMTs with improved breakdown performance

Cite as: Appl. Phys. Lett. **123**, 103502 (2023); doi: 10.1063/5.0169944
Submitted: 30 July 2023 · Accepted: 22 August 2023 ·
Published Online: 6 September 2023

View Online Export Citation CrossMark

JiaQi He,[1,2] KangYao Wen,[1] PeiRan Wang,[1] MingHao He,[1,3] FangZhou Du,[1] Yang Jiang,[1] ChuYing Tang,[1] Nick Tao,[4] Qing Wang,[1,5,a)] Gang Li,[2,a)] and HongYu Yu[1,5,a)]

AFFILIATIONS

[1]School of Microelectronics, Southern University of Science and Technology, Shenzhen 518055, China
[2]Department of Electronic and Information Engineering, The Hong Kong Polytechnic University, Kowloon, Hong Kong
[3]Department of Electrical and Computer Engineering, National University of Singapore, Singapore
[4]Maxscend Microelectronics Company Limited, Wuxi 214072, China
[5]Engineering Research Center of Integrated Circuits for Next-Generation Communications, Ministry of Education, Southern University of Science and Technology, Shenzhen 518055, China

[a)]**Authors to whom correspondence should be addressed:** wangq7@sustech.edu.cn; gang.w.li@polyu.edu.hk; and yuhy@sustech.edu.cn

ABSTRACT

This work adopts interface charge engineering to fabricate normally off metal–insulator–semiconductor high electron mobility transistors (MIS-HEMTs) on an *in situ* SiN_x/AlGaN/GaN platform using an *in situ* O_3 treatment performed in the atomic layer deposition system. The combination of *in situ* SiN_x passivation and an O_3-treated Al_2O_3/AlGaN gate interface allows the device to provide an excellent breakdown voltage of 1498 V at a low specific on-resistance of 2.02 mΩ cm^2. The threshold voltage is increased by 2 V by significantly compensating the net polarization charges by more than five times with O_3 treatment as well as reducing the interface traps and improving the high-temperature gate stability. Furthermore, a physical model of fixed charges at the Al_2O_3/AlGaN interface is established based on dielectric thickness-dependent linear fitting and numerical calculations. The matched device performance and simulated energy band bending elucidate the O_3-treated fixed-charge modulation mechanism, providing a practical method for producing normally off GaN MIS-HEMTs.

GaN metal–insulator–semiconductor high electron mobility transistors (MIS-HEMTs) are potential candidates for the next generation of high-power electronics.[1,2] Generally, the two-dimensional electron gas (2DEG) properties and device performance can be compromised by process-induced damage at the interface of the dielectric/AlGaN barrier. To mitigate this issue, the *in situ* SiN_x insulator layer, which is continuously grown on the AlGaN barrier by metal–organic chemical vapor deposition (MOCVD), has been extensively studied as a means of protecting the AlGaN surface from air and process-induced damage.[3,4] In addition, compared with *ex situ* SiN_x deposition methods, such as plasma-enhanced chemical vapor deposition (PECVD) or low-pressure chemical vapor deposition (LPCVD), *in situ* SiN_x has a lower growth rate and higher growth temperature, which is favorable for reducing dielectric defects, thus suppressing the gate leakage current.[5]

Generally, a large number of positive fixed charges at the *in situ* SiN_x/AlGaN interface induces a high 2DEG density at the AlGaN/GaN heterojunction, and the GaN MIS-HEMT based on the *in situ* SiN_x/AlGaN/GaN platform features a negative threshold voltage (V_{th}) and a low on-state resistance (R_{on}).[6,7] In commercial product applications, the normally on *in situ* SiN_x/AlGaN/GaN MIS-HEMT is usually integrated with a normally off Si MOSFET in a cascode connection to simplify circuit design and build a fail-safe system. The intrinsic parasitic problem in a cascode structure restricts its application to high-frequency and high-voltage fields. As a result, individual etching-free normally off GaN MIS-HEMTs were developed using gate interface engineering and ultrathin-barrier (UTB) techniques by depleting the 2DEG at the gate region.[8–10] It has been reported that the positive fixed charges at the Al_2O_3/GaN interface were decreased by post-dielectric/gate annealing[11] and can also be reduced by a CF_4 or O_2 plasma.[12,13] However, the positive fixed charge at the *in situ* SiN_x/AlGaN interface persists after dry etching unless the underlying AlGaN barrier is simultaneously etched or thinned.[14] Therefore, there are limited reports regarding normally off MIS-HEMT on *in situ* SiN_x/AlGaN/GaN platforms.

This study fabricates a high-performance normally off GaN MIS-HEMT on an *in situ* SiN_x/AlGaN/GaN platform with an Al_2O_3 insulating layer by atomic layer deposition (ALD). An *in situ* O_3 treatment in the ALD system is implemented before the Al_2O_3 deposition to reduce the positive fixed charge on the post-*in situ* SiN_x-etching AlGaN surface. This critical step provides the normally off Al_2O_3/AlGaN/GaN MIS-HEMTs with *in situ* SiN_x passivation, improving the gate and off-state breakdown voltages (*BV*). The conducted dielectric thickness-dependent fitting and simulated models suggest that the O_3 treatment can significantly increase the device V_{th} by compensating for the fixed charges. In addition, both the interface states and high-temperature gate current leakage instability are suppressed in the fabricated normally off GaN MIS-HEMT.

The MIS-HEMTs were fabricated on a 6-inch *in situ* SiN_x/AlGaN/GaN platform. From the bottom to up, it consists of a thick buffer layer, a 300 nm GaN channel layer, a 1 nm AlN spacer, a 5 nm $Al_{0.05}Ga_{0.95}N$ layer, and a 30 nm *in situ* SiN_x cap layer. Because the *in situ* SiN_x strongly passivates the wafer, the device process begins with an Ohmic contact. A Ti/Al/Ti/Au metal stack is evaporated through an opened deposition window, followed by an annealing process at 830 °C for 45 s in an N_2 ambient. Next, the *in situ* SiN_x at the gate region is removed using an inductively coupled plasma reactive ion etching (ICP-RIE) system. After that, the wafer is transferred to the ALD chamber, where it undergoes a pre-gate O_3 treatment at 300 °C. Following this, an 18-nm O_3-based Al_2O_3 insulating layer is deposited, and a Ni/Au metal stack is evaporated as the gate electrode. Subsequently, a 350 °C annealing process is conducted in N_2 ambient for 5 min to improve the Ni/Al_2O_3 contact properties. Finally, a 200-nm SiO_2 layer is deposited by PECVD, and the source field plate is formed to complete the device process.

Figure 1(a) shows the structure of the fabricated GaN MIS-HEMT. The gate width (W_G), gate length (L_G), distance of gate-to-source (L_{GS}), and distance of gate-to-drain were set to 100/2/3/10 μm, respectively, with an extension distance of 3 μm toward the drain side of the source field plate. The main steps of the device process are listed in Fig. 1(b), and an MIS-HEMT without O_3 treatment was also fabricated as a control.

The DC transfer characteristics of the fabricated MIS-HEMTs are plotted in Fig. 2(a) at a bias voltage of $V_D = 10$ V. As shown, the O_3 treatment leads to an increase in the device V_{th} from −1.6 to 0.4 V, which is determined using a drain current criterion of 1 μA/mm. This increase in V_{th} is attributed to the effective reduction of positive fixed charges at the Al_2O_3/AlGaN interface, resulting in a lower net polarization charge density in the gate region.[15,16] The performance of the MIS-HEMTs is also characterized by high extrinsic transconductance, with both values greater than 150 mS/mm, which can be attributed to the excellent gate control ability of the UTB structure.[17] As plotted in Fig. 2(b), the *in situ* SiN_x passivation provides numerous positive fixed charges at the *in situ* SiN_x/AlGaN interface, inducing the high 2DEG density at the UTB $Al_{0.05}Ga_{0.95}N$/GaN heterojunction and excellent output performance. The R_{on} increases from 9.8 to 11.2 Ω·mm, showing a depletion of 2DEG at the gate region for the normally off operation.

The I_G–V_G curve in Fig. 2(c) illustrates that the O_3 treatment allows for a maximum positive V_G of 16 V, while the controlled device shows a limit of only 14.3 V. This slight increase in gate *BV* can be attributed to the lower concentration of oxygen vacancy (V_O) defects resulting from pre-gate O_3 treatment.[18] A similar improvement is seen in the off-state *BV*, which increases from 1278 to 1498 V due to the O_3-treated Al_2O_3/AlGaN interface, as shown in Fig. 2(d). The high-quality *in situ* SiN_x passivation, along with an optimized source field plate, also contributes to the excellent breakdown performance. A 1.5 μm transfer length for each Ohmic contact is included when

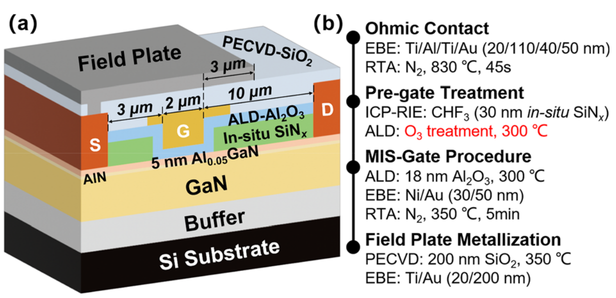

FIG. 1. (a) Schematic of GaN MIS-HEMT on an *in situ* SiN_x/AlGaN/GaN/Si platform; (b) main device fabrication process.

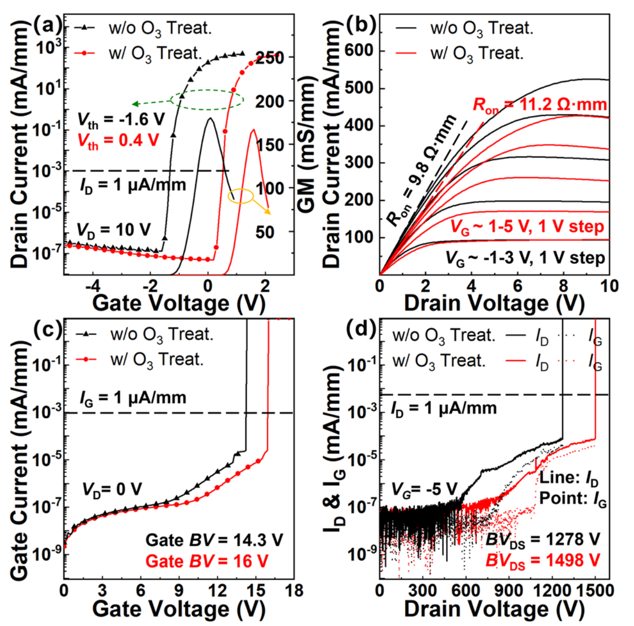

FIG. 2. (a) Semi-log transfer, (b) output, (c) I_G–V_G, and (d) OFF-state characteristics of fabricated GaN MIS-HEMTs on an *in situ* SiN_x/AlGaN/GaN platform without and with O_3 treatment.

calculating specific on-resistance ($R_{on,sp}$), where the optimized device features a high BV_{DS} of 1498 V with a low $R_{on,sp}$ of 2.02 mΩ cm^2.

The reasons for the improved device performance from the O_3 treatment are studied by detecting the microstructure. Figure 3(a) demonstrates the top view and surface profile of the etching trench of *in situ* SiN_x/AlGaN by atomic force microscopy (AFM). Following the removal of *in situ* SiN_x by dry etching, the underlying AlGaN surface displays a root mean square (RMS) roughness of 0.82 nm, while an improved surface morphology with an RMS of 0.54 nm is observed in Fig. 3(b). The O_3 treatment helps to decrease the V_O defects, showing a better pre-deposition surface. Surface X-ray photoelectron spectroscopy (XPS), shown in Fig. 3(c), reveals that Si atoms are present in the top few atomic layers of the AlGaN surface after *in situ* SiN_x etching. The incorporated Si atoms may act as surface donors that significantly impact interface charges and channel scattering.[19] Additionally, after strong oxidization by O_3 treatment, most of the Ga–N and Si–N bonds are replaced by Ga–O and Si–O bonds to form an O-terminated AlGaN surface. Following the Al_2O_3 deposition, scanning transmission electron microscopy [STEM, Fig. 3(d)] shows an apparent local transition layer at the Al_2O_3/AlGaN interface and crystalline grains in the Al_2O_3 bulk, while the cross section of the O_3-treated sample shows

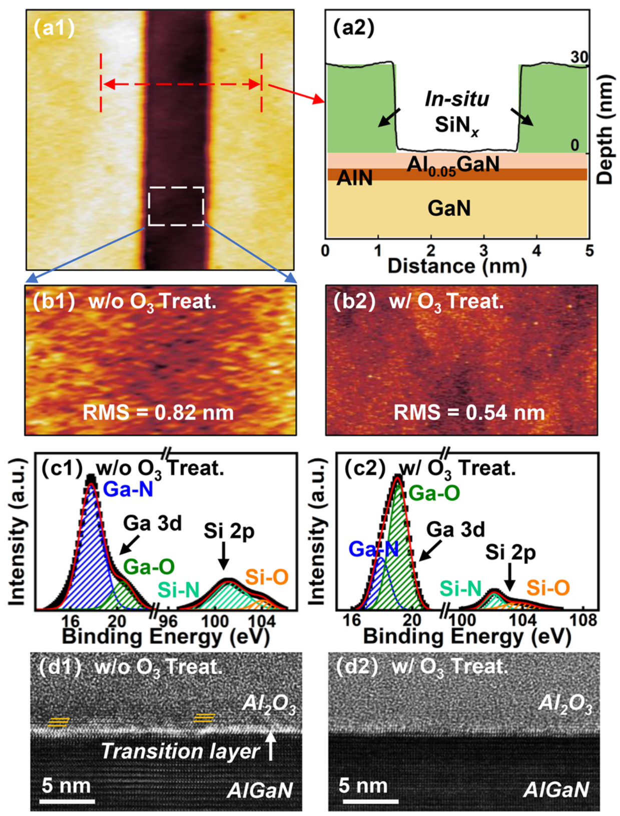

FIG. 3. (a1) AFM top view and (a2) surface profile of *in situ* SiN_x/AlGaN trench; (b) morphology of exposed AlGaN surface after etching and O_3 treatment; (c) XPS analysis of AlGaN surface composition; (d) STEM cross-view of Al_2O_3/AlGaN interface, showing the transition layer (indicated by white arrow) and crystalline grains (highlighted with orange guidelines along the local crystalline orientation) without O_3 treatment.

a sharp interface and amorphous Al_2O_3. The O_3-treated Al_2O_3/AlGaN interface with fewer V_O defects and crystalline grains may suppress the trap-assisted tunneling,[20,21] indicating the improved breakdown performance of GaN MIS-HEMTs in this work.

A series of GaN Schottky HEMTs and MIS-HEMTs with step-graded Al_2O_3 thicknesses were fabricated to confirm the fixed charge variation induced by the O_3 treatment. The V_{th} shift between the GaN MIS-HEMT and Schottky HEMT (no gate dielectric) in this work can be described as[22]

$$\Delta V_{th} = (\Delta\Phi_m - \Delta E_c)/e + (\sigma_F - \sigma_{pol-})/\varepsilon_{Al2O3} \times t_{Al2O3}, \quad (1)$$

where $\Delta\Phi_m$ represents the difference in Schottky barrier height between the Ni/Al_2O_3 and Ni/AlGaN interfaces, ΔE_c is the conduction band offset for Al_2O_3/AlGaN, and σ_F and σ_{pol-} are the Al_2O_3/AlGaN interface fixed charge density and the GaN net negative spontaneous polarization charge density (1.8×10^{13} cm^{-2}), respectively. ε and t are the permittivity and thickness of gate Al_2O_3. The linear fitting in Fig. 4(a) shows that the GaN MIS-HEMT σ_F values with and without O_3 treatment extracted from different slopes are 1.92 and 2.44 $\times 10^{13}$ cm^{-2}, respectively. The net polarization charge densities at the Al_2O_3/AlGaN interface are calculated as 1.2 and 6.4 $\times 10^{12}$ cm^{-2}, indicating that the fixed-charge-induced 2DEG density can be decreased by more than five times by O_3 treatment.

Figure 4(b) plots the double-sweep capacitance–voltage (C–V) curves of the Al_2O_3/$Al_{0.05}$GaN/AlN/GaN MIS-diodes fabricated using the same process as the MIS-HEMTs. The V_{FB} shifts from −1.2 to 0.8 V after O_3 treatment, where the V_{FB} increment of 2 V is in accordance with the MIS-HEMT performance. Furthermore, the C–V hysteresis decreases from 0.55 to 0.04 V, and this remarkable improvement is attributed to the improved Al_2O_3/AlGaN interface quality from the O_3 treatment. The dielectric and interface charges can be extracted from the following equation:[23]

$$Q_t = C_{ox} \times \Delta V_{FB}, \quad (2)$$

where Q_t is the sum of the dielectric bulk and interface trap charges, C_{ox} is the oxide capacitance, and ΔV_{FB} is the flatband voltage shift. The Q_t at the Al_2O_3/AlGaN interface without O_3 treatment is calculated as 1.22×10^{12} cm$^{-2}\cdot$eV^{-1}, while the counterpart O_3-treated interface is 8.62×10^{10} cm$^{-2}\cdot$eV^{-1}. It is confirmed that the bulk and interface traps in the Al_2O_3/AlGaN structure are effectively reduced by more than one order of magnitude by the O_3 treatment. Furthermore, the gate current leakage increases with increasing test temperature. The gate BV degenerates from 14.3 to 12 V at 200 °C, while the O_3-treated device features a stabilized gate current leakage with the maximum gate voltage decreasing by less than 1 V, as plotted in Fig. 4(c). Thus, the temperature-dependent, trap-assisted tunneling or Poole–Frenkel emission is suppressed in the O_3-treated interface, demonstrating high-temperature gate stability for the fabricated GaN MIS-HEMT.

According to the microstructure and device characteristics, the atom arrangements of the *in situ* SiN_x/AlGaN interface and Al_2O_3 fabricated on the post-*in situ* SiN_x-etching AlGaN surface are illustrated in Figs. 5(a)–5(c). V_O defects and substitutional Si atom dangling bonds at the O_3-treated Al_2O_3/AlGaN interface are both compensated, reducing the traps and positive fixed charges. The decreased interface charges (Q_{it}) and oxide bulk charges ($Q_{ox,\ bulk}$) trapped in the MIS

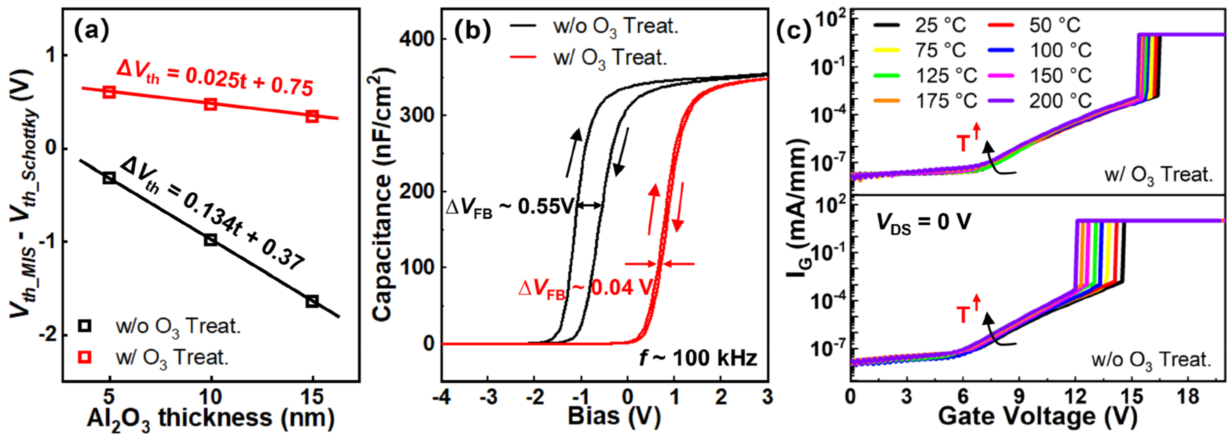

FIG. 4. (a) Experimental V_{th} shift and linear fitting between GaN MIS-HEMT and Schottky HEMT vs various gate Al_2O_3 thicknesses; (b) double-sweep *C–V* characteristics of $Al_2O_3/Al_{0.05}GaN/AlN/GaN$ MIS-diode at $f = 100$ kHz; and (c) temperature-dependent gate current leakage.

structure contribute to improving the breakdown performance, while the reduced positive fixed charge (σ_F) increases the V_{th} of GaN MIS-HEMT.

The main charge distribution is demonstrated in Fig. 5(d), considering the polarization charges (σ_{AlGaN}, $\sigma_{AlGaN/AlN}$, and $\sigma_{AlN/GaN}$) in the $Al_2O_3/Al_{0.05}GaN/AlN/GaN$ gate stack. By calculating the heterojunction polarization charges from Vegard's law[24] and applying the σ_F ranging from 2.44 to $1.92 \times 10^{13}\,cm^{-2}$ in this work, the simulated energy band bending is depicted in Fig. 5(e). The bottom of the conduction band (E_C) at the AlGaN/AlN/GaN interface rises above the Fermi level (E_F) by reducing the positive fixed charge, matching the device operation to shift from normally on to normally off. The physical model of the Al_2O_3 thickness-dependent linear fitting and numerical simulation reveals the significance of fixed-charge modulation of V_{th} in GaN MIS-HEMTs.

Using O_3 treatment by ALD, a method for interface charge engineering is adapted to a UTB AlGaN/GaN MIS-HEMT with *in situ* SiN_x caps. A physical relation is established between the interface properties of Al_2O_3/AlGaN and charge variation induced by *in situ* SiN_x etching/O_3 treatment through XPS analysis, AFM/TEM characterization, *C–V* measurement, and energy band simulation. The O_3-treated Al_2O_3/AlGaN boundary charges are compensated by five times, and the interface traps are reduced by more than one order of magnitude. The fixed-charge modulation resulted in the relatively small positive V_{th} of 0.4 V for normally off operation on GaN MIS-HEMTs. To satisfy the demands of high-power switching system, the V_{th} is assumed to be further increased by optimizing the temperature of O_3 treatment and the post-dielectric/metallization-annealing (PDA/PMA) processes. Meanwhile, combining a high-quality Al_2O_3/AlGaN gate interface with *in situ* SiN_x passivation enables the device to display an excellent *BV* of 1498 V with a low $R_{on,sp}$ of 2.02 mΩ cm^2. The *in situ* O_3 treatment during the ALD procedure provides a practical method for fabricating normally off GaN power HEMTs with excellent breakdown performance.

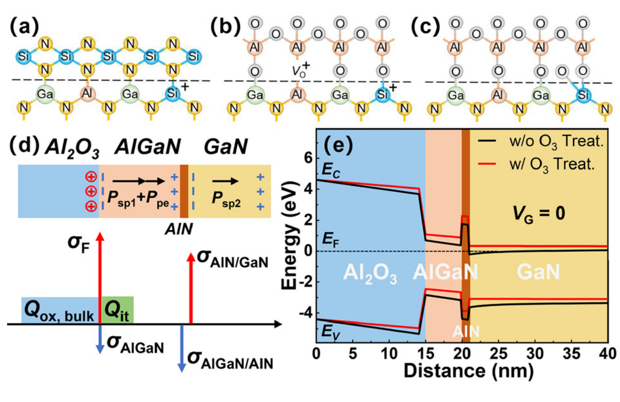

FIG. 5. Illustration of atomic arrangements for (a) *in situ* SiN_x/AlGaN interface. Al_2O_3/AlGaN interfaces (b) without and (c) with O_3 treatment after etching *in situ* SiN_x. (d) Schematic distribution profile of relevant charges in the $Al_2O_3/Al_{0.05}GaN/AlN/GaN$ gate stack. (e) Calculated energy band diagrams for this work considering the σ_F of 1.92×10^{13} (red) and $2.44 \times 10^{13}\,cm^{-2}$ (black) at the $Al_2O_3/Al_{0.05}GaN$ interface.

This work was supported by the National Natural Science Foundation of China (Grant No. 62122004), Research on the Fabrication and Mechanism of GaN Power and RF Devices (Grant No. JCYJ20200109141233476), Study on the Reliability of GaN Power Devices (Grant No. JCYJ20220818100605012), Research on the GaN Chip for 5G Applications (Grant No. JCYJ20210324120409025), and Research on High-Reliable GaN Power Device and the Related Industrial Power System (Grant No. HZQB-KCZYZ-2021052).

AUTHOR DECLARATIONS

Conflict of Interest

The authors have no conflicts to disclose.

Author Contributions

Jiaqi He: Conceptualization (lead); Formal analysis (lead); Investigation (lead); Methodology (lead); Writing – original draft (lead). **Kangyao Wen:** Data curation (supporting); Formal analysis (supporting). **Peiran Wang:** Software (supporting). **Minghao He:** Formal analysis (supporting); Methodology (supporting). **Fangzhou**

Du: Resources (supporting). **Yang Jiang:** Methodology (supporting); Validation (supporting). **Chuying Tang:** Project administration (supporting). **Nick Tao:** Writing – review & editing (supporting). **Qing Wang:** Funding acquisition (supporting); Project administration (supporting); Supervision (supporting); Writing – original draft (supporting). **Gang Li:** Methodology (supporting); Supervision (supporting); Validation (supporting). **Hongyu Yu:** Funding acquisition (lead); Project administration (lead); Supervision (lead); Writing – review & editing (lead).

DATA AVAILABILITY

The data that support the findings of this study are available from the corresponding author upon reasonable request.

REFERENCES

[1]M. Meneghini, C. D. Santi, I. Abid, M. Buffolo, M. Cioni, R. A. Khadar, L. Nela, N. Zagni, A. Chini, F. Medjdoub, G. Meneghesso, G. Verzellesi, E. Zanoni, and E. Matioli, J. Appl. Phys. **130**(18), 181101 (2021).

[2]J. He, W.-C. Cheng, Q. Wang, K. Cheng, H. Yu, and Y. Chai, Adv. Electron. Mater. **7**(4), 2001045 (2021).

[3]L. Cheng, W. Xu, D. Pan, Y. Zhu, F. Ren, D. Zhou, J. Ye, D. Chen, R. Zhang, and Y. Zheng, J. Phys. D **52**(30), 305105 (2019).

[4]X. Lu, J. Ma, H. Jiang, C. Liu, P. Xu, and K. M. Lau, IEEE Trans. Electron Devices **62**(6), 1862 (2015).

[5]M. Tadjer, T. Anderson, K. Hobart, M. Mastro, J. Hite, J. Caldwell, Y. Picard, F. Kub, and C. Eddy, J. Electron. Mater. **39**(11), 2452 (2010).

[6]H. Jiang, C. Liu, Y. Chen, X. Lu, C. W. Tang, and K. M. Lau, IEEE Trans. Electron Devices **64**(3), 832 (2017).

[7]P. Moens, C. Liu, A. Banerjee, P. Vanmeerbeek, P. Coppens, H. Ziad, A. Constant, Z. Li, H. De Vleeschouwer, and J. Roig-Guitart, in paper Presented at the 2014 IEEE 26th International Symposium on Power Semiconductor Devices & IC's, 2014.

[8]S. Huang, X. Wang, X. Liu, Y. Wang, J. Fan, S. Yang, H. Yin, K. Wei, W. Wang, and H. Gao, Appl. Phys. Express **12**(2), 024001 (2019).

[9]R. Zhao, S. Huang, X. Wang, Y. Li, J. Shi, Y. Zhang, J. Fan, H. Yin, X. Chen, K. Wei, S. Wu, X. Yang, B. Shen, and X. Liu, Appl. Phys. Lett. **116**(10), 142105 (2020).

[10]A. Endoh, Y. Yamashita, K. Ikeda, M. Higashiwaki, K. Hikosaka, T. Matsui, S. Hiyamizu, and T. Mimura, Jpn. J. Appl. Phys., Part 1 **43**(4S), 2255 (2004).

[11]Q. Zhou, Y. Yang, K. Hu, R. Zhu, W. Chen, and B. Zhang, IEEE Trans. Ind. Electron. **64**(11), 8971 (2017).

[12]H.-C. Wang, T.-E. Hsieh, Y.-C. Lin, Q. H. Luc, S.-C. Liu, C.-H. Wu, C. F. Dee, B. Y. Majlis, and E. Y. Chang, IEEE J. Electron Devices Soc. **6**, 110 (2018).

[13]N. Sun, H. Huang, Z. Sun, R. Wang, S. Li, P. Tao, Y. Ren, S. Song, H. Wang, S. Li, W. Cheng, and H. Liang, IEEE Trans. Electron Devices **69**(1), 82 (2022).

[14]J. He, W.-C. Cheng, Y. Jiang, M. Fan, G. Zhou, G. Yang, L. Jiang, X. Wang, Z. Wu, Q. Wang, and H. Yu, Mater. Sci. Semicond. Process. **132**, 105907 (2021).

[15]S.-C. Liu, C.-K. Huang, C.-H. Chang, Y.-C. Lin, B.-Y. Chen, S.-P. Tsai, B. Y. Majlis, C.-F. Dee, and E. Y. Chang, IEEE J. Electron Devices Soc. **5**(3), 170 (2017).

[16]T. Kubo, M. Miyoshi, and T. Egawa, Semicond. Sci. Technol. **32**(6), 065012 (2017).

[17]S. Huang, X. Wang, X. Liu, Q. Sun, and K. J. Chen, Semicond. Sci. Technol. **36**(4), 044002 (2021).

[18]W.-C. Cheng, J. He, M. He, Z. Qiao, Y. Jiang, F. Du, X. Wang, H. Hong, Q. Wang, and H. Yu, J. Vac. Sci. Technol. B **40**(2), 022212 (2022).

[19]H. Guo, P. Shao, C. Zeng, H. Bai, R. Wang, D. Pan, P. Chen, D. Chen, H. Lu, R. Zhang, and Y. Zheng, Appl. Surf. Sci. **590**, 153086 (2022).

[20]E. J. Miller, E. T. Yu, P. Waltereit, and J. S. Speck, Appl. Phys. Lett. **84**(4), 535 (2004).

[21]H. Zhang, E. J. Miller, and E. T. Yu, J. Appl. Phys. **99**(2), 023703 (2006).

[22]Z. Liu, S. Huang, Q. Bao, X. Wang, K. Wei, H. Jiang, H. Cui, J. Li, C. Zhao, X. Liu, J. Zhang, Q. Zhou, W. Chen, B. Zhang, and L. Jia, J. Vac. Sci. Technol. B **34**(4), 041202 (2016).

[23]S. Huang, S. Yang, J. Roberts, and K. J. Chen, Jpn. J. Appl. Phys., Part 1 **50**, 110202 (2011).

[24]O. Ambacher, J. Majewski, C. Miskys, A. Link, M. Hermann, M. Eickhoff, M. Stutzmann, F. Bernardini, V. Fiorentini, and V. Tilak, J. Phys. **14**(13), 3399 (2002).